

RESEARCH PAPER

## Preparation Nanostructured of Cu-Doped NiO Thin Films Using Spin Coating Method for Gas Sensors Applications

Hajer T. Hashim <sup>1</sup>, Mahdi M. Mutter <sup>2\*</sup>, Souad G. Khalil <sup>1</sup>, and Ghassan A. Naeem <sup>3</sup>

<sup>1</sup> Department of Physics, College of Science for Women, University of Baghdad, Baghdad, Iraq

<sup>2</sup> Center of Applied Physics, Material Research Department, Ministry of Science and Technology, Baghdad, Iraq

<sup>3</sup> Department of Biophysics, College of Applied Science, University of Anbar, Anbar, Iraq

### ARTICLE INFO

#### Article History:

Received 28 June 2022

Accepted 16 September 2022

Published 01 October 2022

#### Keywords:

AFM

Copper-doped

NiO thin films

Optical properties

Sensing properties

Sol-gel technique

XRD

### ABSTRACT

In this paper, copper doped nickel oxide as the thin films have been synthesized by a sol-gel spin coating method for gas sensing application. The ratios of Cu -doped were (1, 2, and 3) %wt. The characterization of obtained films was investigated in detail of the structural, morphological surface, optical properties, and sensing properties of Nitrogen dioxide (NO<sub>2</sub>) and hydrogen sulfide (H<sub>2</sub>S) gases. The crystallinity was confirmed by the x-ray diffraction (XRD) analyses. The surface morphology is characterized by atomic force microscopy (AFM). The NiO: Cu films have a polycrystalline with a cubic structure phase. The results of AFM showed the roughness and grain size distribution decreased from (13.56-22.71) nm, and (2.56-5.21) nm, respectively. The optical property showed that the highest absorption of the obtained films was 0.739 to the 1%Cu sample and the bandgap decreased from (3.31 to 3.01) eV with increasing Cu doped. The results of sensing analysis showed the doping of NiO film with Cu was suitable for gas sensing applications where the electrical conductivity of NiO was an enhancement.

### How to cite this article

Hashim H T., Mutter M M., Khalil S G., Naeem G A. Preparation Nanostructured of Cu-Doped NiO Thin Films Using Spin Coating Method for Gas Sensors Applications. J Nanostruct, 2022; 12(4):882-891. DOI: 10.22052/JNS.2022.04.010

### INTRODUCTION

Semiconductors are important materials, which have made significant progress, have made the extent of the last decade, inherited extensively through a range of electronic applications and devices, including electronic devices, optical guests, light-emitting, photocatalysis, and other applications [1]. Nickel oxide (NiO) is a semiconductor p-type; it has a cube structure, as well thin films, and good transparency. NiO has been used in many applications because of its crystal good and best permeability of a wide

range of visible wavelengths, also, possessing an energy gap between (3.6 to 4) eV [2]. These thin films of NiO are used in many applications such as solar cells, chemical sensors, electric minors, photovoltaic, organic-relief diodes, and UV detection devices[3]. Hydrogen sulfide (H<sub>2</sub>S) is a flammable gas and its properties are colorless with a distinctive smell of rotten eggs. This gas naturally produces volcanic lava and some water from the well and is also produced when the bacteria decompose organic matter in the absence of oxygen. It has been widely observed

\* Corresponding Author Email: [dorkoosh@tums.ac.ir](mailto:dorkoosh@tums.ac.ir)



by the  $H_2S$  gas in industrial places. Consequently, workers in these environments may be exposed to  $H_2S$  gas, as well as workers in agriculture, oil, and wastewater treatment, and the dangerous dose of this gas that causes death when exposed to it is  $H_2S$  (>500 ppm)[4]. Nitrogen dioxide ( $NO_2$ ) is one of the numerous nitrogen oxides. It is a gas in its natural state, brown-red color has a sharp permeable smell.  $NO_2$  is one of the most important and most common air pollutants and causes poisoning when inhaled. Traffic emissions are the main source of nitrogen oxides while some small concentrations are produced from power stations and some other industrial sources, but emissions from power stations and industrial areas are in most cases high on the monitoring stations and their rise helps the speed of the spread of pollutants in the atmosphere, so traffic emissions are the main source and the dangerous dose of this gas that causes death when exposed to it is  $H_2S$  (>100 ppm)[5]. Several deposition methods can get NiO thin films like as, electrochemical deposition, Pulsed laser deposition (PLD), plasma sputtering, thermal evaporation, Sol-Gel process, and chemical vapor deposition (CVD) [6][7]. The semiconductor applications problems are high values of energy gaps and the lack of electrical conductivity so many researchers seek to improve the physical properties of these materials through vaccination with other elements. In this work, we synthesis undoped and doped NiO by Cu as thin films by using sol-gel spin coating method for gas sensing application. The target gases were  $NO_2$  and  $H_2S$  with operating temperature (200, 250,

and 300) °C, also the structure properties, surface morphology, optical properties were investigated.

## MATERIALS AND METHODS

### Materials

Nickel acetate tetrahydrate powder ( $C_4H_6NiO_4 \cdot 4H_2O$ ) purity at 99.99%, 2-methoxyethanol ( $C_3H_8O_2$ ) purity at 99.00%, and Monoethanolamine (MEA) purity at 98% were used as stabilizer and solvent. Copper nitrate  $Cu(NO_3)_2$  was used as a source of Cu doped. The substrate used was Glass. All starter materials were supplied from Sigma-Aldrich, Malaysia.

### Preparation of NiO: Cu thin films

Nickel acetate tetrahydrate powder was dissolved in 2-methoxyethanol with a solution concentration of 0.5 M. The solution was mixed by using magnetic stirred for 30 minutes and 60 °C, after 30 minutes a drop of MEA was added to the solution, and then the solution lasts for another 30 minutes until the solution is becoming clear. To make Cu doping it's prepared by the same condition. The two solutions were mixed according to ratios of Cu-doping (1,2, and 3) wt%. The prepared solution was left for aging at room temperature for 24 hours, to allow forming the gel to complete hydrolysis [8]. The deposition process of NiO: Cu films by using a spin coater, Model VTC-100. The preparation process of the films has done in three steps: first at 500 rpm for 5 seconds, the second at 1000 rpm for 30 seconds, and at 3000 rpm for 5 minutes. The drying films at 80 °C for 15 minutes by using the oven to evaporate

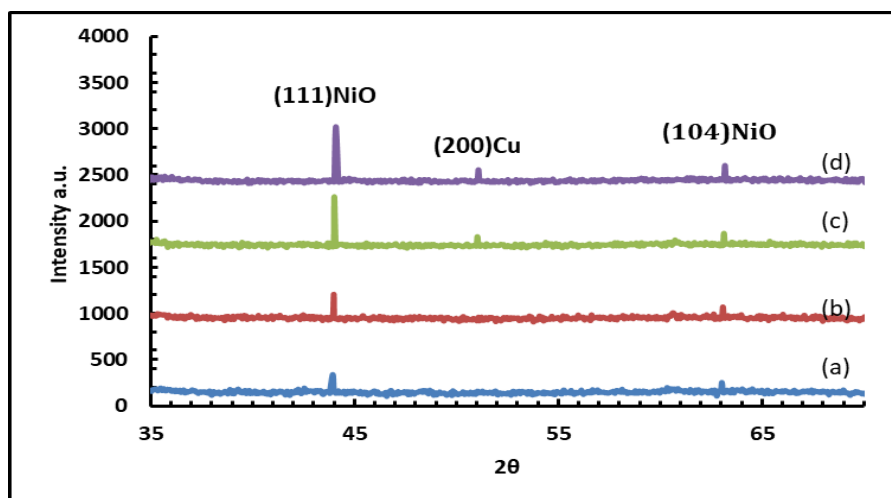


Fig. 1. XRD patterns of NiO: Cu films, (a) NiO, (b) doping 1%Cu, (c) doping 2%Cu, (d) doping 3%Cu."

Table 1 Microstructure properties of NiO: Cu films

NiO: Cu films	2θ (Deg.)	ε	D (nm)	δ=1/D <sup>2</sup> (line.nm <sup>-2</sup> )	α
0%Cu	43.925	0.002	48.1502	0.0004	0.0019
1%Cu	43.975	0.002	48.4036	0.0004	0.0019
2%Cu	43.025	0.002	48.5492	0.0004	0.0019
3%Cu	43.710	0.027	19.2477	0.0019	0.0019

the solvent and remove organic matter. This process is repeated five times to get the required thickness. Thereafter, the obtained films were annealed at 450 °C for 2 hours. Before deposition, the glass substrate was cleaned using acetone, methanol, and de-ionized water, an ultrasonic cleaner. For thickness measurement a fizeau method was used for this purpose, the obtained thicknesses were (189, 230, 210.4, and 197.8) nm for NiO, 1% Cu, 2%Cu, 3%Cu, respectively. Shimadzu XRD 6100/7000, λCuKα = 0.15406 nm) was used for structure properties analysis, atomic force microscopy (AFM) used type (Nitegra NT. MDT), the scan electronic microscopy (SEM) was type JEOL, 67001 and UV-visible (35-LAMBDA) for measurement of optical properties.

**RESULTS AND DISCUSSION**

Fig. 1 showed the X-ray diffraction pattern of the NiO: Cu films with Cu-doping ratios (1 to 3) wt% and annealing at 450 °C for two hours. XRD patterns showed peaks at 43.92° and 63.12°, corresponding to the (111) and (104) planes, which describe a polycrystalline for the cubic

structure phase of NiO, respectively, according to the JCPDS file no. 04-0835. Fig. 1 showed a simple shift in the angles of NiO film of the other samples, and the samples, 2%Cu and 3%Cu doping were appearances a peak indicated to copper phase at the angle 43.02 and (111) plane, according to the JCPDS file no. 04-0936. The average crystalline size was measured by using the Debye–Scherrer equation [9]:

$$D = \frac{0.9\lambda}{\beta \cos \theta\beta} \tag{1}$$

Where D: the crystallite size (nm), λ: x-ray wavelength (1.54 Å), β: the FWHM width of the peak, and θ<sub>β</sub>: the diffraction angle of the peak.

Moreover, microstrain (ε), dislocation density (δ), and stacking fault probability (α) were measured by the equations [10-11]:

$$\delta = \frac{1}{D^2} \tag{2}$$

$$\epsilon = \left( \frac{|CoICDD - CoXRD|}{CoICDD} \right) \times 100 \tag{3}$$

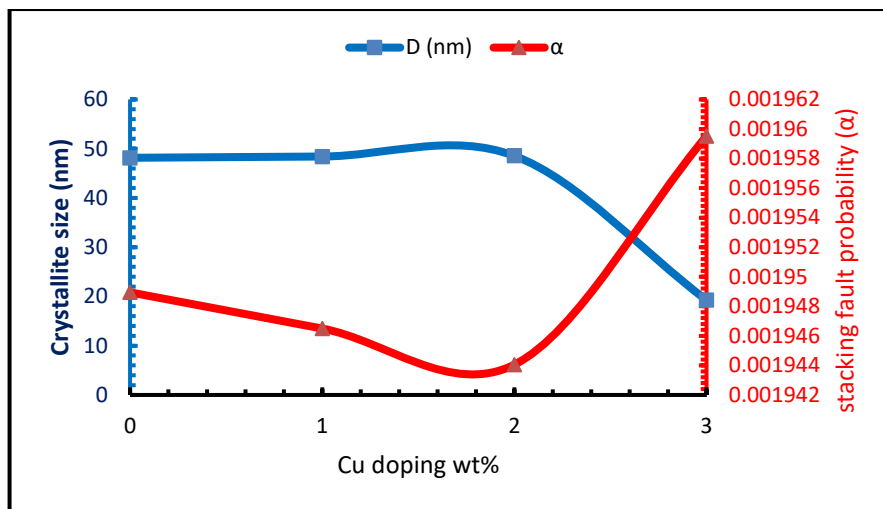


Fig. 2. Crystalline size and stacking fault probability of NiO: Cu films with Cu-doping ratios.

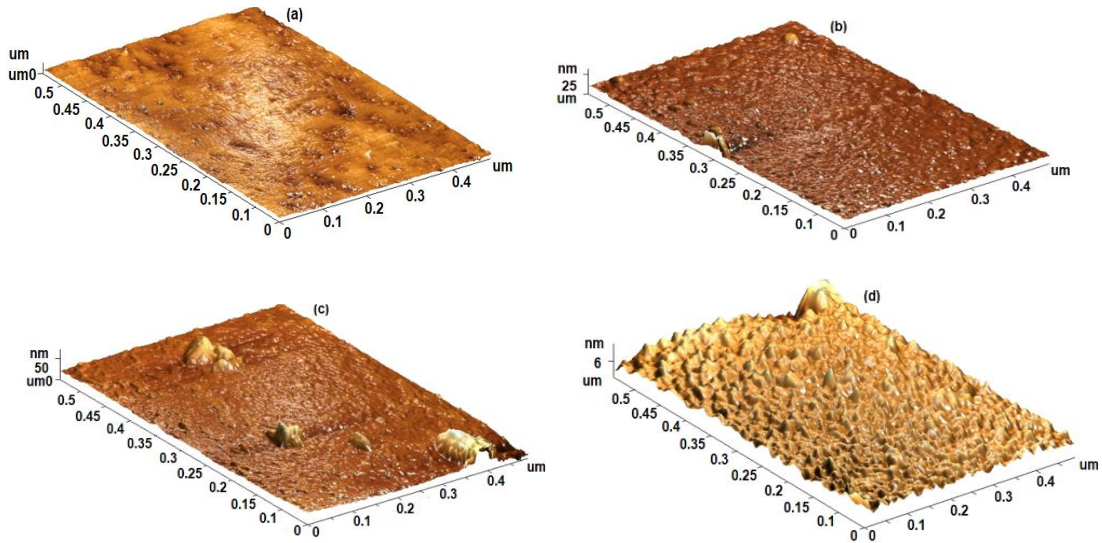


Fig. 3. AFM images NiO: Cu films, (a) 0%Cu-doped, (b) NiO:1%Cu-doped, (c) NiO:2%Cu-doped, (d) NiO:3%Cu-doped.

$$\alpha = \frac{2\pi 2\Delta(2\theta)}{45 \tan \theta} \quad (4)$$

Where  $C_{ICDD}$ : lattice constant, ICDD and  $C_{XRD}$ : value forth lattice constant. The result showed an enhancement in crystallinity of NiO: Cu films compared with the results of many researchers[7-10]. Table 1 summarizes the results of the XRD data analysis.

Fig. 2 showed the crystalline sizes (D) and stacking fault probability ( $\alpha$ ) of NiO: Cu films as a function of Cu-doping concentration. The crystalline size was decreased with an increase

in Cu concentration, also, the stacking fault probability increased with increasing Cu-doping, This suggests that Cu atoms in the NiO structure may restrict the grain growth of NiO films due to the lowest ionic radius of  $Cu^{2+}(0.69 \text{ \AA})$  than  $Ni^{2+}(0.72 \text{ \AA})$ , also, the stacking fault probability is directly proportional to the crystallization, as the less crystallization, the more randomness, and thus the decreased in the values of the stacking fault probability, this is agreed with the results of [12].

Fig. 3 showed AFM images of the surface

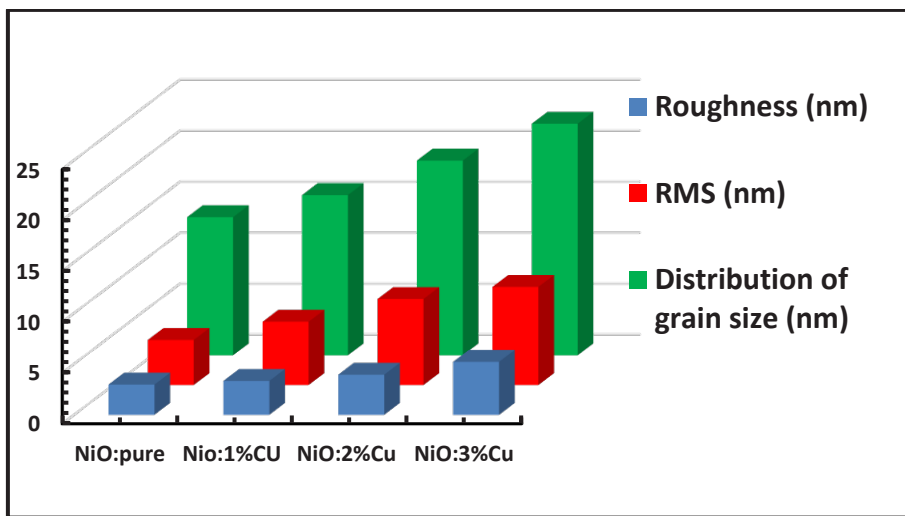


Fig. 4. Histogram of results NiO: Cu films for AFM images.

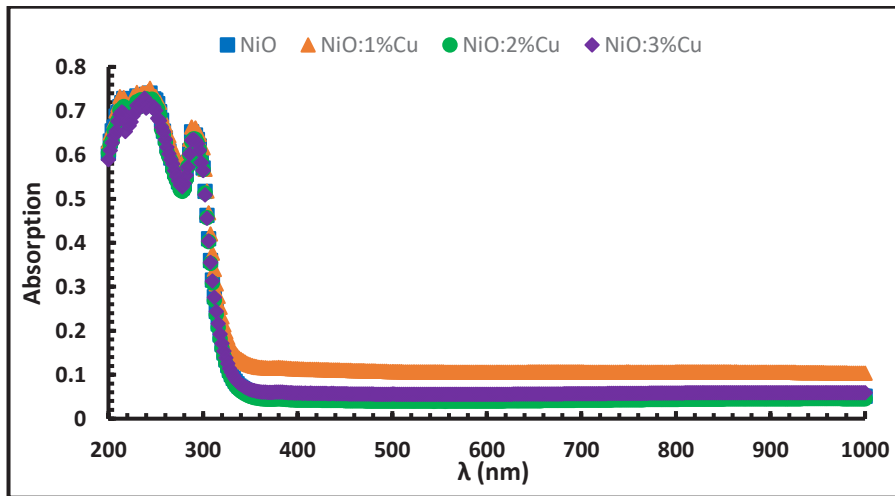


Fig. 5. UV- Visible absorption diagrams of the NiO: Cu films at different Cu-doping.

morphology for NiO: Cu films, the scanning images (4.5x4.5)  $\mu\text{m}$  of the film surfaces for all samples, and the images of the prepared films were in (3-D). The grain size distribution of the surface increased (13.576 to 22.724) nm with increasing the ratios of Cu-doped. Fig. 4 showed the results analysis of AFM images. It observed that the roughness and root mean square (RMS) of the NiO sample was (2.937) nm and (4.436) nm respectively, and then it's increased to (5.211) nm and (9.653) nm with increased the Cu content. The reason for these increases in the value of roughness and RMS can be attributed to the increase in the Cu-doping, where the difference between  $\text{Cu}^{+2}$  and the  $\text{Ni}^{+3}$  is

the latest increase in the roughness and RMS [13].

This technique of UV-Visible is described that fact shows the electron is moved from band to band, where it moved from valence band to conductivity band when the electron acquires the energy necessary to cross the energy gap of the semiconductor. The electrons move occurred because the absorption of photons provides rich information on the transition type. When an electron momentum is saved that the transition is immediately and is not measured by indirect energy and the transition power is measured by using the relation of  $T_{auc}$  [14]. Fig. 5 showed the absorption spectra of NiO: Cu films at different

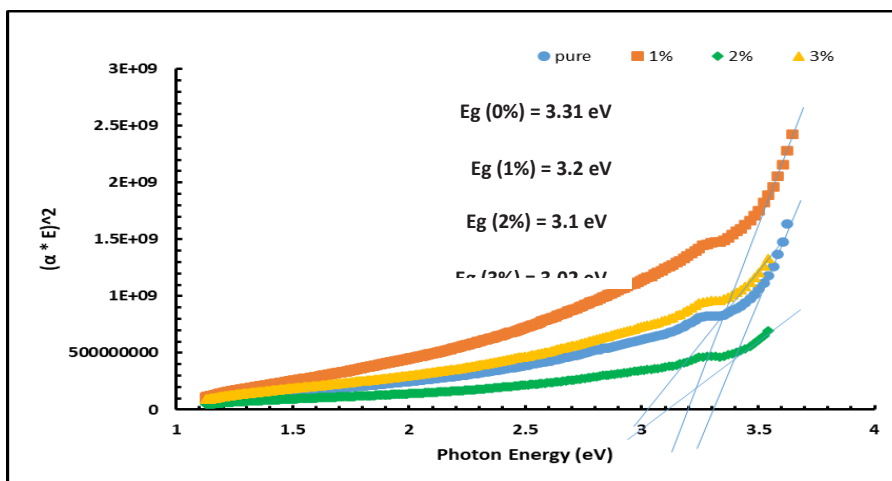


Fig. 6. The energy gap of the NiO: Cu films.

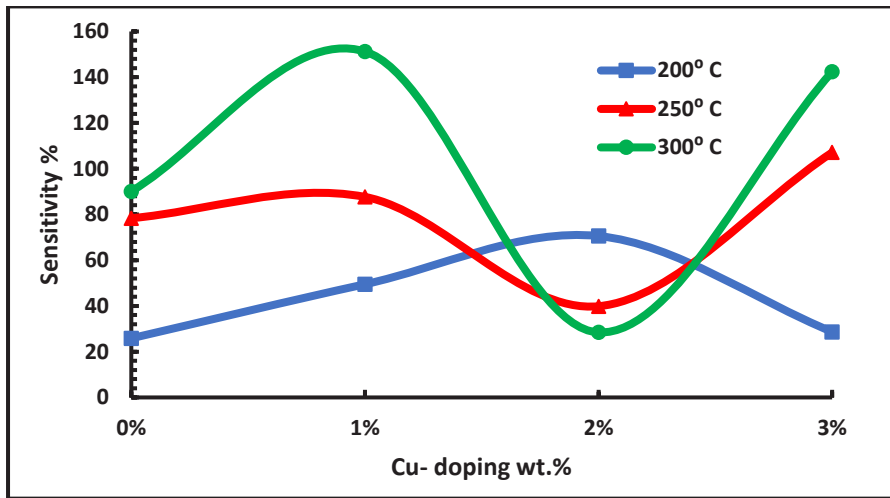


Fig. 7. The sensitivity of NiO:Cu films with Cu concentration at different operating temperatures for H<sub>2</sub>S gas.

ratios of Cu-doping (1,2 and 3) %wt percentage. The behavior of absorption spectra was turned towards the higher wavelength of absorption edges with an increase of Cu-doped. This shift showed decreasing in values of bandgap as shown in Fig. 6, this is because of an increase in the particle size [15]. The measured value of absorption edges of NiO: Cu obtained films at different ratios of 330, 336, 339, and 340 nm for NiO, 1%Cu, 2%Cu, and 3%Cu respectively. Also, Fig. 5 shows an exponential decrease in the absorption pattern with increasing wavelength.

There are many reasons, including the interaction of photons with the internal electric fields within the crystal volume of the prepared films, and the deformation that occurs to the lattice because the strain caused by the deficiency and inelastic scattering occurs for charge carriers by phonons [16]. The absorption coefficient ( $\alpha$ ) related to the absorption area of the prepared films was calculated from the equation below [17]:

$$\alpha = \frac{2.303A}{t} \quad (5)$$

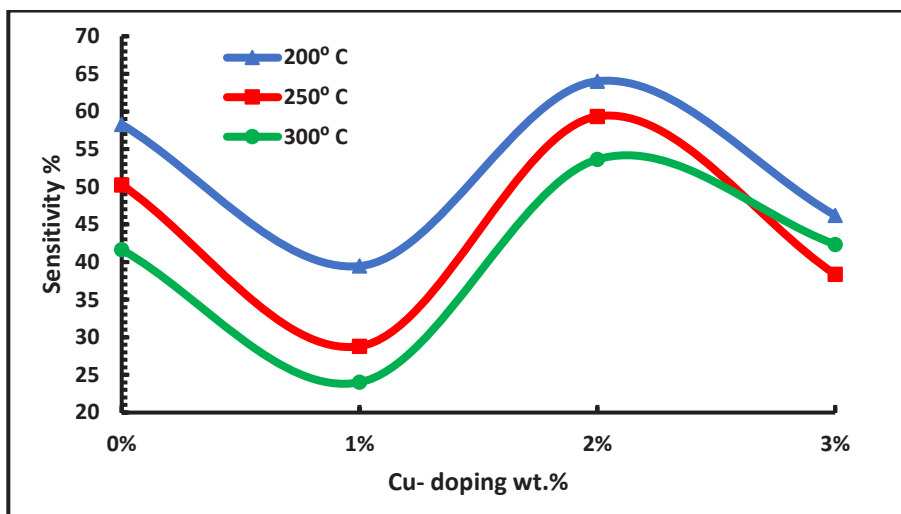


Fig. 8. The sensitivity of NiO:Cu films with Cu concentration at different operating temperatures for NO<sub>2</sub> gas.

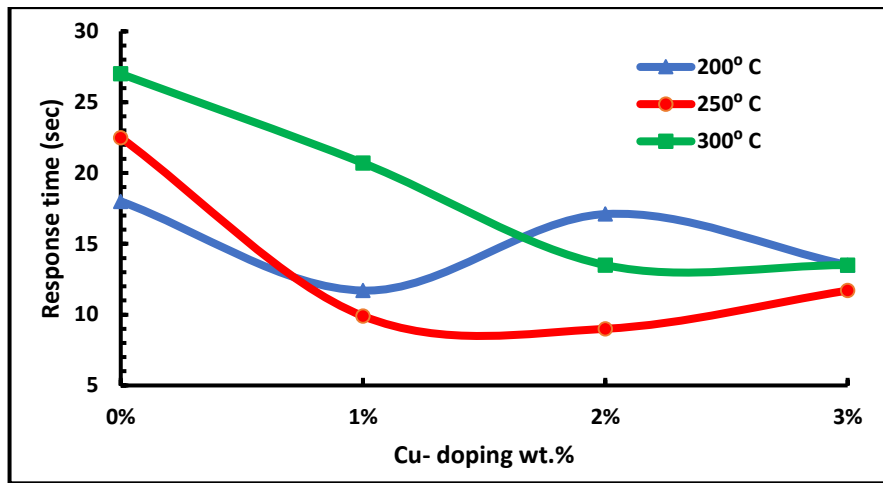


Fig. 9. Response time of NiO: Cu films for H<sub>2</sub>S gas.

Where:  $\alpha$ : absorption coefficient, A: absorption and t: thickness.

the energy gap ( $E_g$ ) of prepared films measured by used Tauc formal [18]:

$$(\alpha hv)^n = B(hv - E_g) \quad (6)$$

Where ( $\alpha, hv$ ): absorption coefficient, photo energy, respectively, B is a constant belonging to the material and n equal 2 or 1/2 for direct and indirect bandgap respectively. The optical bandgap is measured by concluding the linear part of the  $(\alpha hv)^n - hv$  curve as shown in Fig.6.

Fig. 6 showed the energy gap of NiO: Cu films. The number linear relation was for  $n = 1/2$ , suggesting that NiO: Cu films are a semiconductor

with direct transition [19]. The values of energy gap were (3.31, 3.2, 3.1, and 3.02) eV for NiO,1%Cu, 2%Cu, and 3%Cu, respectively.

The sensitivity% can be defined as the ratio between changing the resistance of the sensor with the presence of gas and without gas [20]:

$$S\% = \frac{G_g - G_a}{G_a} \quad (7)$$

Where  $G_a$ : the resistance of sensor in air,  $G_g$ : the resistance of sensor in presence of a gas. The target gases were NO<sub>2</sub> as an oxidized gas and H<sub>2</sub>S as a reduced gas.

Fig. 7 shows the sensitivity% of NiO: Cu films at present H<sub>2</sub>S gas. The sensitivity in general increased with increasing Cu content and

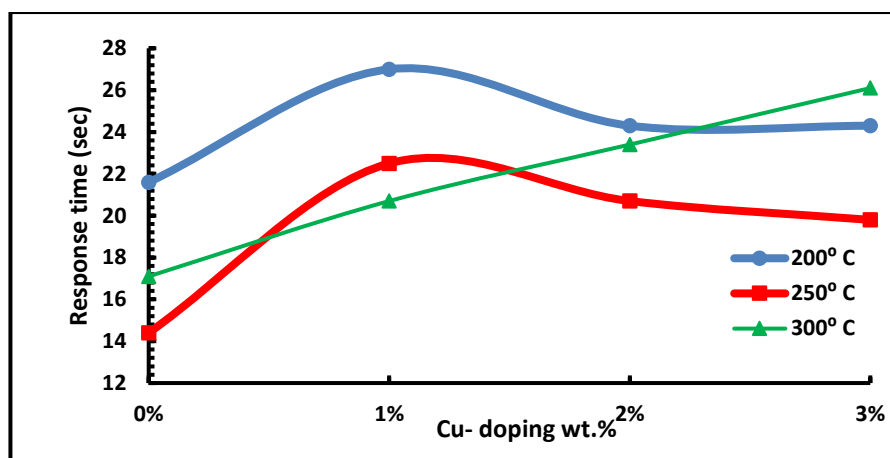


Fig. 10. Response time of NiO: Cu films for NO<sub>2</sub> gas.

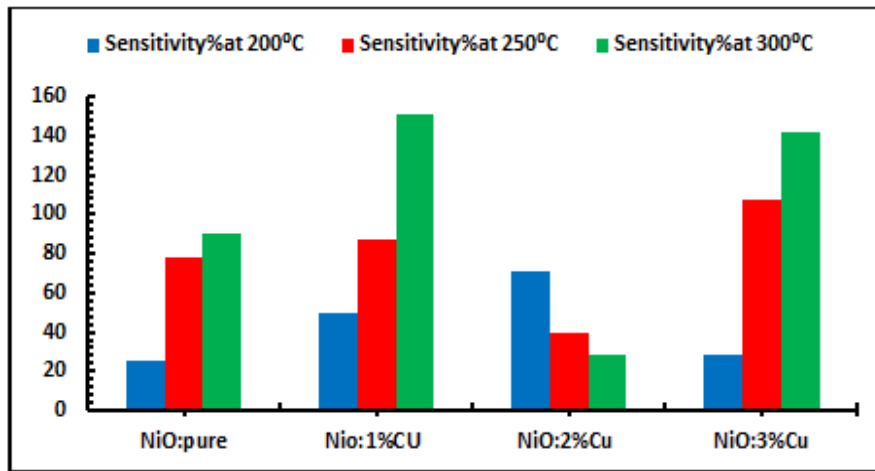


Fig. 11. Histogram of the sensitivity% values of NiO: Cu films for H<sub>2</sub>S gas.

operator temperature, as for the pure sample NiO film, the sensitivity% increased by increasing the temperature, and the reason for this is due to the nature of the semiconductor material, as its resistance is decreased by increasing the temperature and thus an increase in the sensitivity [21], as for the 1%Cu sample, the sensitivity% was also increasing with an increase in the temperature, and the reason for this positive effect of heat on-resistance of semiconductor with metal [22]. While the 2%Cu sample the sensitivity% was completely different from the rest of the samples and the reason, for this may be due to the bad homogeneity in this sample.

The sensitivity% of the 3%Cu sample was also increased with an increase in the temperature because of the positive affect of heat on resistance of semi-conductor with metal.

Fig. 8 illustrates another behavior of NiO: Cu films with NO<sub>2</sub> gas, In the pure sample NiO film, the sensitivity% decreased by increasing the temperature, and the reason for this is due to the nature of the semiconductor p-type, as its resistance is known to act usually as oxidation gas on n-type metal-oxide semiconductors [23]. Also, the sensitivity of the other samples decreased with an increase in the operating temperature, but this is a different effect from one sample to

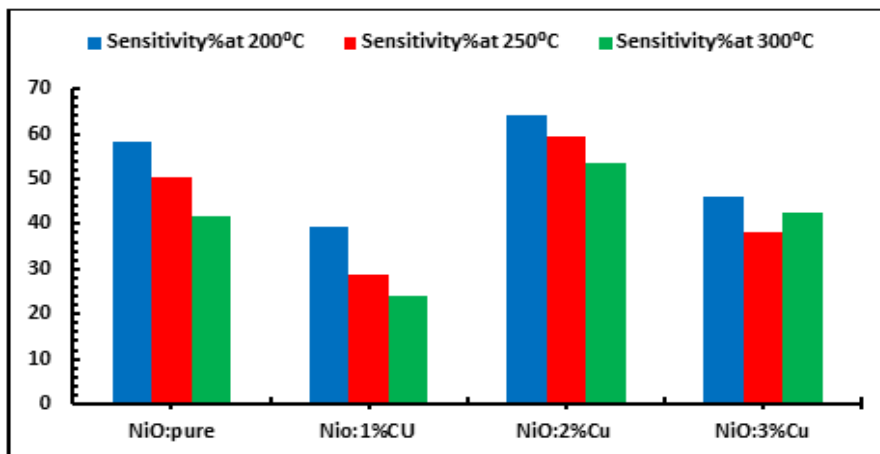


Fig. 12. Histogram of the sensitivity% values of NiO: Cu films for NO<sub>2</sub> gas.

another, the reason for this is due to the nature of the crystallization of the prepared samples, as well as the influence of the resistance of the semiconductors of the n-type with oxidizing gases [24]

Fig. (9,10) showed The response time of H<sub>2</sub>S and NO<sub>2</sub> gases, respectively. Fig. 9 showed the response time of the pure sample was increased with an increase in temperature and this is due to the effect of temperature on the resistivity of the prepared film [23]. As for the rest samples (1%,2%, and 3%)Cu, the time of response with the temperatures is irregular, and the reason for this is due to the lack of homogeneity of the metal-doped on the surface of the samples [25]. Fig. 10 showed the response time of NiO: Cu films for NO<sub>2</sub> gas. It is clear that the response time with the temperatures is irregular, and the reason for this is due to the lack of homogeneity of the metal-doped on the surface of the samples and the nature of act the oxidizing gases on the resistivity of the semiconductors from n-type [24].

Fig. 11 showed histogram of the sensitivity% values of NiO: Cu films with the temperatures for H<sub>2</sub>S gas. The results illustrated that the best sensitivity% was to NiO:1%Cu films at 300° C. Fig. 12 summarizes the results of sensitivity% values of NiO: Cu films with the temperatures for NO<sub>2</sub> gas, the results showed that the best sensitivity% was NiO:2%Cu films at 200 °C.

## CONCLUSION

The sol-gel spin coating technique was used to prepare NiO: Cu thin films at different ration of Cu (1,2, and 3)wt% as a gas sensor of two gases H<sub>2</sub>S and NO<sub>2</sub>. The results of XRD illustrated that NiO: Cu thin films exhibit Poor crystallization the phase was monoclinic, and the crystallite size increased from (48.15024 to 19.24775) nm with increasing Cu-doped concentration. AFM images revealed that the grain size distribution on the surface of prepared samples increased from (13.56 to 22.72) nm with increased Cu-doped. Optical absorption results indicate a low absorbance in the infrared and visible regions and the bandgap of NiO film was 3.31 eV, while it's reduced to (3.2, 3.1, and 3.02) eV for Cu-doped at 1%, 2%, and 3%, respectively. The gas sensor results of NiO: Cu films, the results indicate that the best sensitivity to H<sub>2</sub>S gas was NiO:1%Cu film, where the sensitivity % was 151.24% at 300 °C and the best sensitivity to NO<sub>2</sub> was NiO:2%Cu film, where the sensitivity %

was 64.03% at 200 °C. We conclude that NiO: Cu films are potential sensors for H<sub>2</sub>S and NO<sub>2</sub>, with a strong response to H<sub>2</sub>S gas.

## CONFLICT OF INTEREST

The authors declare that there is no conflict of interests regarding the publication of this manuscript.

## REFERENCES

1. Napari M, Huq TN, Hoyer RLZ, MacManus-Driscoll JL. Nickel oxide thin films grown by chemical deposition techniques: Potential and challenges in next-generation rigid and flexible device applications. *InfoMat*. 2020;3(5):536-576.
2. Benramache S, Benhaoua B, Guezoun H. Study the Effect of Cu Doping on Optical and Structural Properties of NiO Thin Films. *Annals of West University of Timisoara - Physics*. 2020;62(1):15-22.
3. Guezoun H. Synthesis and Characterizations of Nanocrystalline Na and Al Codoped NiO Thin Films. *International Journal of Integrated Engineering*. 2020;12(1).
4. Aroca A, Gotor C, Bassham DC, Romero LC. Hydrogen Sulfide: From a Toxic Molecule to a Key Molecule of Cell Life. *Antioxidants*. 2020;9(7):621.
5. Low Temperature Sensing Of NO<sub>2</sub> Gas Using SnO<sub>2</sub>-ZnO Nanocomposite Sensor. *Advanced Materials Letters*. 2013;4(3):196-201.
6. Chtouki T, Soumahoro L, Kulyk B, Erguig H, Elidrissi B, Sahraoui B. Spin-coated Tin-doped NiO thin films for third order nonlinear optical applications. *Optik*. 2017;136:237-243.
7. Boulila S, Ghamnia M, Boukhachem A, Ouhaibi A, Chakhoum MA, Fauquet C, et al. Photocatalytic properties of NiO nanofilms doped with Ba. *Philos Mag Lett*. 2020;100(6):283-293.
8. Farrag AA-G, Balboul MR. Nano ZnO thin films synthesis by sol-gel spin coating method as a transparent layer for solar cell applications. *J Sol-Gel Sci Technol*. 2016;82(1):269-279.
9. Al-Rashedi K, Farooqui M, Rabbani G. Characterizing Crystalline Chromium oxide Thin Film Growth by Sol-gel method on Glass Substrates. *Oriental Journal of Chemistry*. 2018;34(4):2203-2207.
10. Kulkarni S, Patil D. Effect of Firing Temperature on Electrical and Structural Characteristics of Screen Printed In<sub>2</sub>O<sub>3</sub> Thick Films. *DEStech Transactions on Environment, Energy and Earth Science*. 2016(seeie).
11. Mahmood A, Naeem A. Sol-Gel-Derived Doped ZnO Thin Films: Processing, Properties, and Applications. *Recent Applications in Sol-Gel Synthesis: InTech*; 2017.
12. Aoun Y, Marrakchi M, Benramache S, Benhaoua B, Lakel S, Cherif A. Preparation and Characterizations of Monocrystalline Na Doped NiO Thin Films. *Materials Research*. 2018;21(2).
13. Gurakar S, Serin T, Serin N. Electrical And Microstructural Properties Of (Cu, Al, In)-doped SnO<sub>2</sub> Films Deposited By Spray Pyrolysis. *Advanced Materials Letters*. 2014;5(6):309-314.
14. Dressel M, Grüner G. *Electrodynamics of Solids*: Cambridge University Press; 2002 2002/01/17.
15. Dharmaraj N, Prabu P, Nagarajan S, Kim CH, Park JH, Kim HY. Synthesis of nickel oxide nanoparticles using nickel acetate

- and poly(vinyl acetate) precursor. *Materials Science and Engineering: B*. 2006;128(1-3):111-114.
16. Kumar H, Rani R. Structural and Optical Characterization of ZnO Nanoparticles Synthesized by Microemulsion Route. *International Letters of Chemistry, Physics and Astronomy*. 2013;19:26-36.
17. Klick CC. The Optical Properties of Solids. Course 34, International School of Physics "Enrico Fermi," 1965. J. Tauc, Ed. Academic Press, New York, 1966. 448 pp., illus. \$22. *Science*. 1967;158(3804):1038-1038.
18. Khashan KS, Sulaiman GM, Abdulameer FA. Synthesis and Antibacterial Activity of CuO Nanoparticles Suspension Induced by Laser Ablation in Liquid. *Arabian Journal for Science and Engineering*. 2015;41(1):301-310.
19. Song X, Gao L. Facile Synthesis of Polycrystalline NiO Nanorods Assisted by Microwave Heating. *J Am Ceram Soc*. 2008;91(10):3465-3468.
20. Khalil, et al. Fabrication and Characterization of Gas Sensor from ZrO<sub>2</sub>: MgO Nanostructure Thin Films by R.F. Magnetron Sputtering Technique. *Baghdad Science Journal*. 2019;16(1):0199.
21. Rydosz A. The Use of Copper Oxide Thin Films in Gas-Sensing Applications. *Coatings*. 2018;8(12):425.
22. Kılıç A, Alev O, Özdemir O, Arslan LÇ, Büyükköse S, Öztürk ZZ. The effect of Ag loading on gas sensor properties of TiO<sub>2</sub> nanorods. *Thin Solid Films*. 2021;726:138662.
23. Hotový I, Rehacek V, Siciliano P, Capone S, Spiess L. Sensing characteristics of NiO thin films as NO<sub>2</sub> gas sensor. *Thin Solid Films*. 2002;418(1):9-15.
24. Deng Y. Sensing Mechanism and Evaluation Criteria of Semiconducting Metal Oxides Gas Sensors. *Semiconducting Metal Oxides for Gas Sensing*: Springer Singapore; 2019. p. 23-51.
25. Hotový I, Huran J, Spiess L, Čapkovic R, Haščík Š. Preparation and characterization of NiO thin films for gas sensor applications. *Vacuum*. 2000;58(2-3):300-307.